Paper 70-3 has been designated as a Distinguished Paper at Display Week 2025. The full-length version of this paper appears in a Special Section of the *Journal of the Society for Information Display (JSID)* devoted to Display Week 2025 Distinguished Papers. This Special Section will be freely accessible until December 31, 2025 via:

https://sid.onlinelibrary.wiley.com/doi/full/10.1002/jsid.2084

Authors that wish to refer to this work are advised to cite the full-length version by referring to its DOI:

https://doi.org/10.1002/jsid.2084

Hydrogen-free Oxide Thin-Film Transistor Toward Resolving Hydrogen-Associated Instability

Mamoru Furuta*, Mir Mutakabbir Alom*, Motoki Ando*,
***Kochi University of Technology, Kochi, Japan**
Yoshihiro Sato**, Takafumi Kambe**, and Tsutomu Satoyoshi**
****Tokyo Electron Technology Solutions Ltd., Yamanashi, Japan**

Abstract

We propose and demonstrate the concept of hydrogen-free (H-free) amorphous oxide semiconductor thin-film transistor (AOS TFT) to resolve hydrogen-associated instability of the TFT. H-free SiO_2 and SiNx films were successfully deposited by large-area inductively coupled plasma chemical vapor deposition (ICP-CVD) using hydrogen-free source gases. Both films were applied as the gate insulator and passivation layers of the TFT, respectively. The H-free In–Ga–Zn–Sn–O (IGZTO) TFT showed field-effect mobility of 23.2 cm^2/Vs and excellent stability under positive gate bias stress for 7200 s at stress temperatures in the range of 60–100 °C.

Author Keywords

Amorphous Oxide Semiconductors (AOS), Thin-Film Transistor (TFT), In–Ga–Zn–Sn–O (IGZTO), Reliability, Hydrogen-Free AOS TFT.

1. Introduction

Amorphous oxide semiconductors (AOS) have attracted attention for their use in an active channel layer of thin-film transistors (TFT) due to their high field effect mobility (μ_{FE}>10 $cm^2V^{-1}s^{-1}$), large area uniformity, and extremely low off current.[1,2] The application of oxide TFT has expanded to low temperature poly-Si (LTPS) and oxide (LTPO) TFTs[3] for low power consumption organic light-emitting diode (OLED) displays due to an extremely low off current of oxide TFTs. There are two types of LTPO stack-up processes with bottom- and top-gate AOS TFTs. The top-gate AOS TFT is preferred for the LTPO TFT because the LTPS and the AOS TFTs can be optimized independently. Moreover, to take advantage of the unique characteristics of AOS TFT, the self-aligned top-gate (SATG) structure is essential to reduce parasitic capacitance in the TFT. To manage the reliability of the LTPO TFTs, hydrogen-associated instability of the AOS TFT should be considered.[3]

For the SATG AOS TFT, both the gate insulator (GI) and the passivation layers are key materials that guarantee the performance and reliability of the TFT. A GI of SiO_2 is commonly deposited by plasma-enhanced chemical vapor deposition (PE-CVD) on the AOS channel using hydrogen-contained SiH_4/N_2O or $TEOS/O_2$ source gases. Because large amounts of hydrogen are incorporated into both the GI and the AOS channel during SiO_2 GI deposition,[4] a low hydrogen SiO_2 deposition recipe was applied to the GI deposition of the AOS TFT.[5,6] However, the GI still contained hydrogen around 10^{21} cm^{-3}, which is comparable to H in the AOS channel, even deposited by a low hydrogen deposition recipe. Furthermore, the passivation layer of the SiN_x film also contained large amounts of hydrogen more than 10^{21} cm^{-3}. The hydrogen in the GI and passivation layers will diffuse into the AOS channel during the TFT fabrication and annealing processes, resulting in influence on the performance and the reliability of the TFT. To manage the reliability of AOS TFT and understand the hydrogen-associated degradation mechanism, it is essential to realize hydrogen-free (H-free) AOS TFT.

In this presentation, H-free SiO_2 and SiN_x are successfully deposited by newly developed large-area inductively coupled plasma CVD (ICP-CVD) using hydrogen-free source gases to demonstrate the H-free AOS TFT with high mobility In–Ga–Zn–Sn–O (IGZTO) channel. The IGZTO TFT showed field effect mobility (μ_{FE}) of 23.2 $cm^2V^{-1}s^{-1}$ with excellent stability under positive and negative gate bias stresses (PBTS and NBTS) at a stress temperature of 60 °C.

2. Experiment and Results

2.1 Fabrication Process of Self-Aligned Top-Gate IGZTO TFT

Figure 1 shows the schematic cross-sectional image and the fabrication process step of the SATG IGZTO TFT.

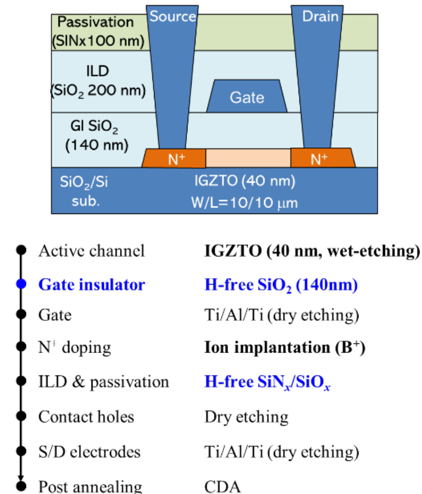

Figure 1. Schematic cross-sectional image and fabrication process steps of SATG IGZTO TFT.

The IGZTO TFT was fabricated on a SiO_2 coated Si substrate. First, a 40-nm thick amorphous IGZTO was deposited by sputtering. After channel isolation by wet etching, the IGZTO channel was annealed in clean dry air (CDA) at 350 °C for 1 h. A 140-nm thick H-free SiO_2 layer was deposited by ICP-CVD at 300 °C for the gate insulator (GI) and annealed in CDA at 300 °C

ISSN 0097-996X/25/5602-0954-$1.00 © 2025

for 1 h. The Ti/Al/Ti stacked film was then deposited on GI and patterned into gate electrodes by dry etching. Boron ions were implanted through the GI to the IGZTO film to form the source and drain (SD) regions in a self-aligned manner. Then 200-nm thick H-free SiO_2 and 100-nm thick H-free SiN_x films were sequentially deposited without breaking vacuum by ICP-CVD at 350 °C for interlayer dielectric (ILD) and passivation layers, respectively. Note that all of the GI, ILD, and passivation layers were deposited by hydrogen-free source gases. After contact holes were opened, SD electrodes were formed by stacked film of Ti/Al/Ti. Both the channel length and the width of the TFT were 10 µm, which were defined by the photolithography process. Finally, the IGZTO TFTs were annealed in CDA at 330 °C for 1 h prior to electrical measurements.

2.2 Control of hydrogen in SiO2 for H-free AOS TFT

The concept of H-free AOS TFT reduces the H concentration in the SiO_2 and the SiN_x films for the GI, ILD, and passivation layers to less than that in the AOS channel to suppress the hydrogen-associated instability in the AOS TFT.

The hydrogen profile in both the IGZTO and the SiO_2 GI was evaluated by secondary ion mass spectrometry (SIMS). The IGZTO film was deposited on Si substrate by sputtering. While SiO_2 films were deposited on Si substrate by ICP-CVD using SiH_4 and N_2O source gas (SiH_4/N_2O) or hydrogen free source gas (H-free). For the SiH_4/N_2O-SiO_2 film, two different deposition recipes (low and high ICP power) were used to control the H concentration in the film.

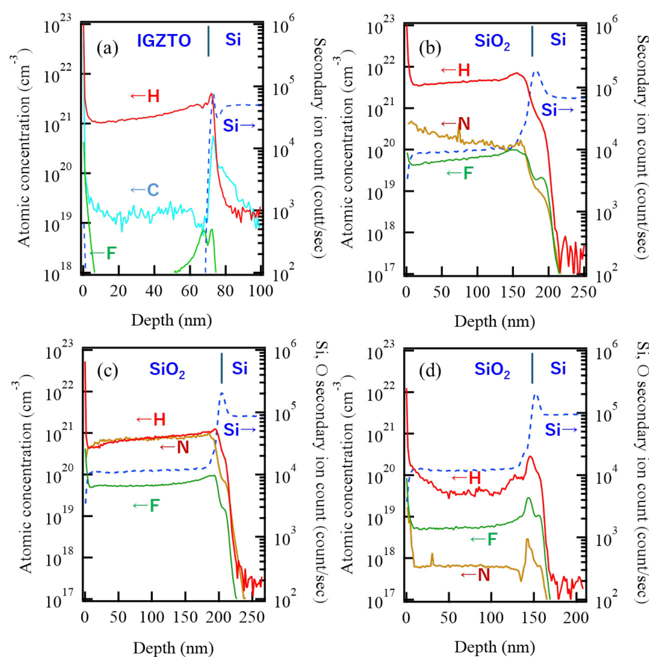

Figure 2. (a) SIMS depth profiles of hydrogen (H), carbon (C), and fluorine (F) in IGZTO film on Si. Depth profiles of H, F, and nitrogen (N) in SiH_4/N_2O-based SiO_2 on Si deposited by ICP-CVD using deposition recipes with (b) low and (c) high ICP powers. (d) Depth profiles of H, F, and N in SiO_2 on Si deposited by ICP-CVD using hydrogen-free source gases.

Figure 2(a) shows the result of the SIMS depth analysis of hydrogen (H), carbon (C), and fluorine (F) in the IGZTO film. Atomic concentrations of H and C in the IGZTO film were 1.4×10^{21} cm^{-3} and 1×10^{19} cm^{-3}, respectively. Since the IGZTO film was deposited by sputtering in Ar and O_2 gases, the H in the IGZTO film mainly originated from the residual water at the base pressure of the sputtering chamber. The F in the IGZTO film was less than 1×10^{18} cm^{-3}.

Figures 2(b) and 2(c) show the depth profiles of H, F, and nitrogen (N) in the SiH_4/N_2O-SiO_2 films deposited by ICP-CVD using (b) low and (c) high ICP power deposition recipes, respectively. Although the H content in the film could be reduced by increasing the ICP power during deposition, the H in the SiH_4/N_2O-SiO_2 film remained 1×10^{21} cm^{-3}. Additionally, there is a trade-off between H and N concentration in the SiH_4/N_2O-SiO_2 film. The high-power deposition recipe reduced H but increased N concentration in the film. The F in the films were mainly derived from the residual chamber cleaning gas in the CVD chamber.

Figure 2(d) shows the depth profiles of H, F, and N in the H-free SiO_2 film deposited by the hydrogen-free source gas. Both H and F concentration in the H-free SiO_2 film was reduced by more than one order magnitude compared to the SiH_4/N_2O-SiO_2 film (Fig. 2(b) and (c)). Since the H concentration in H-free SiO_2 (3×10^{19} cm^{-3}) is approximately two orders of magnitude less than that in the IGZTO channel, hydrogen-associated degradation of the IGZTO channel will be suppressed during the deposition of H-free SiO_2 GI on the AOS channel. The N concentration in the H-free SiO_2 film was more than three orders of magnitude less than that in the SiH_4/N_2O-SiO_2 films. In addition, the H-free SiN_x film is also developed for the passivation layer of the TFT. The H concentration in the SiN_x passivation film was evaluated to be 2×10^{19} cm^{-3}. The H concentration in both the SiO_2 and SiN_x are more than two orders of magnitude lower than that in the IGZTO channel.

With the development of the H-free SiO_2 for the GI layer and the H-free SiN_x for the passivation layer, hydrogen diffusion into the AOS channel during the TFT fabrication process and post-fabrication annealing does not need to be considered.

2.3 Electrical Properties of IGZTO TFT

Figure 3 and Table I show the transfer characteristics and summary of electrical properties of the SATG H-free IGZTO TFT.

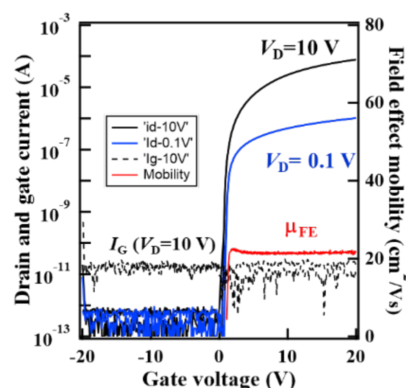

Figure 3. Transfer characteristics of SATG IGZTO TFT.

Table I. Summary of electrical properties of the H-free IGZTO TFTs.

IGZTO TFT	μ_{FE} (cm^2/Vs)	V_{th} (V)	*S.S.* (V/dec.)	V_{Hys} (V)
H-free	23.2	1.08	0.10	0.02

The IGZTO TFT showed good switching properties and operated in enhancement mode with threshold voltage (V_{th}) of 1.08 V. The subthreshold swing (*S.S.*) of 0.10 V/dec. was obtained without hysteresis. The lack of hysteresis and the good *S.S.* value of the TFT indicate a good interface property between the H-free GI and the IGZTO channel. Gate leakage current (I_G at V_D of 10 V) was also shown in Fig. 3. Field effect mobility (μ_{FE}) was extracted from transconductance in a linear region (V_D of 0.1 V). μ_{FE} of 23.2 $cm^2V^{-1}s^{-1}$ was obtained.

2.4 Reliability of H-free IGZTO TFTF

The mobility-stability trade-off has been reported in AOS TFTs especially under negative gate bias stress (NBS).[7, 8] The conduction band minimum (E_{CBM}) tends to deepen with an increase of the contribution of 5*s* orbitals in In or Sn, resulting in a reduction in an effective mass of electron and an increase of μ_{FE} of the TFT. On the other hand, the activation energy of dopants will decrease, and carrier doping ability will increase when In or Sn content in AOS increases. As a consequence, negative V_{th} shifts are often observed under NBS due to Fermi level shift in high-mobility amorphous and polycrystalline OS TFTs.[7-10] In contrast, positive V_{th} shifts are commonly reported from AOS TFT under positive gate bias stress (PBS) due to electron trapping at the GI/AOS interface or in the GI.[11] Therefore, it is of greatest importance to understand the influence of hydrogen on the V_{th} stability of AOS TFTs. The reliability of the IGZTO TFT was evaluated under positive and negative gate bias and temperature stress (PBTS and NBTS).

Figures 4(a) and 4(b) show the evolution of the transfer characteristics under PBTS and NBTS, respectively, at a stress temperature of 60 °C. Positive and negative gate bias stress of +20V and -20V were applied for 7200 s under PBTS and NBTS, respectively. As shown in Figs. 4(a) and 4(b), the SATG H-free IGZTO TFT showed good reliability under both PBTS and NBTS at a stress temperature of 60 °C. In particular, no change of the V_{th} value was observed under PBTS. On the other hand, although negative V_{th} shift is often observed under the NBTS for both amorphous and polycrystalline oxide TFTs[7-10], a positive V_{th} shift of +0.17 V was observed after NBTS for 7,200 s. To further understand the reliability and degradation mechanism of the high-mobility IGZTO TFTs, their PBTS and NBTS reliabilities were evaluated at stress temperatures in the range of 60–100 °C.

Figures 4(c) and 4(d) show the V_{th} shift values (ΔV_{th}) as a function of stress time under PBTS and NBTS, respectively, at stress temperatures in the range of 60–100 °C. Table II summarizes ΔV_{th} values under PBTS and NBTS for 7200 s at each stress temperature.

The H-free IGZTO TFT exhibited excellent PBTS reliability at stress temperatures in the range of 60–100 °C. No V_{th} shift (ΔV_{th} of less than 0.1 V) was observed under PBTS for 7200 s even at a stress temperature of 100 °C, as shown in Fig. 4(c). The PBTS results indicate that electron traps at the GI/IGZTO interface were suppressed in the H-free IGZTO TFT. For the case of the SiO_2 GI deposition using SiH_4/N_2O source gases, H-related chemical species were generated in the vapor phase by the dissociation of SiH_4 gas. The generated H-related chemical species reacted with AOS surface and generated oxygen vacancies and electron traps at the GI/AOS interface during SiO_2 GI deposition. In contrast, GI in the H-free IGZTO TFT was deposited using H-free source gas. Because no H-related chemical species were generated in the vapor phase during the SiO_2 GI deposition for the H-free IGZTO TFT, the H-related reduction reaction at the AOS surface was suppressed, resulting in the formation of an excellent GI/AOS interface without electron traps and hysteresis in transfer characteristics. This is an important result of the concept of H-free AOS TFTs.

On the other hand, the amount of positive V_{th} shift increased with the stress temperature under NBTS, as shown in Fig. 4(d). A plausible reason for the positive V_{th} shift under the NBTS would be the electron trapping phenomenon at the back-channel interface.[12, 13] Electrons in the sub-gap states were excited by the stress temperature and trapped at the back-channel interface under negative gate electric field, resulting in a positive V_{th} shift under the NBTS. Therefore, understanding the positive V_{th} shift mechanism under NBTS is important for future research to further improve the reliability of AOS TFTs.

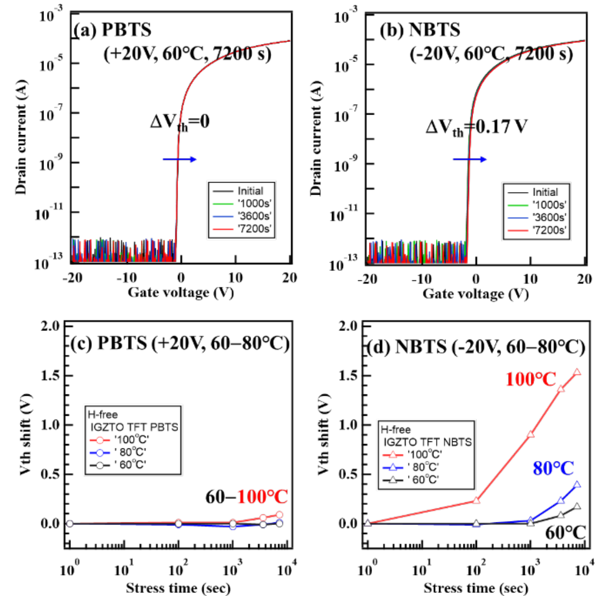

Figure 4 Evolution of transfer characteristics of IGZTO TFT under (a) PBTS and (b) NBTS at a stress temperature of 60 °C. Stress time dependence of V_{th} shift under (c) PBTS and (d) NBTS at stress temperatures in the range of 60–100 °C.

Table II. V_{th} shift under PBTS and NBTS after 7200 s at stress temperature from 60 to 100 °C.

	ΔV_{th} after 7200 s stress			
	Stress temp.	60 °C	80 °C	100 °C
H-free IGZTO TFT	PBTS	0.00	0.01	0.09
	NBTS	0.17	0.39	1.53

3. Conclusion

We proposed and demonstrated the H-free AOS TFT to suppress the hydrogen-associated instability of the TFT. Through the development of H-free SiO_2 and SiN_x films, which were deposited by large-area ICP-CVD using hydrogen-free source gases, the H concentration in the films could be reduced by two orders of magnitude compared with those in the IGZTO channel. The H-free IGZTO TFT showed μ_{FE} value of 23.2 $cm^2V^{-1}s^{-1}$ without hysteresis. The IGZTO TFT exhibited excellent stability in PBTS. No change in V_{th} was observed under PBTS at stress temperatures in the range of 60 – 100 °C. These results indicate that the H-free GI contributed to a marked improvement in the interface quality of the GI/AOS channel because no H-related chemical species were generated in the vapor phase during H-free SiO_2 GI deposition on the AOS, resulting in the suppression of the H-related chemical reduction reaction at the GI/AOS interface. H-free AOS TFT play a key role in achieving highly stable AOS TFT, particularly high-mobility AOS TFT.

References

1. Nomura, K., Ohta, H., Takagi, A., Kamiya, T., Hirano, M., and Hosono, H., Room-temperature fabrication of transparent flexible thin-film transistors using amorphous oxide semiconductors. Nature **432**, 488–492 (2004). https://doi.org/10.1038/nature03090
2. Kato, K., Shionoiri, Y., Sekine, Y., Furutani, K., Hatano, T., Aoki, T., Sasaki, M., Tomatsu, H., Koyama, J., and Yamazaki, S., Evaluation of Off-State Current Characteristics of Transistor Using Oxide Semiconductor Material, Indium–Gallium–Zinc Oxide. Jpn. J. Appl. Phys., **51** 021201(2012). http://dx.doi.org/10.1143/JJAP.51.021201
3. Chang, T., Lin, C. and Chang, S. (2019), 39-3: *Invited Paper:* LTPO TFT Technology for AMOLEDs†. SID Symposium Digest of Technical Papers, **50**: 545-548. https://doi.org/10.1002/sdtp.12978
4. Noh, H.Y., Lee, WG., G. R., H. *et al.* Hydrogen diffusion and its electrical properties variation as a function of the IGZO stacking structure. *Sci Rep* **12**, 19816 (2022). https://doi.org/10.1038/s41598-022-24212-7
5. Toda, T., Wang, D., Jiang, J., Hung, M. P., and Furuta, M., "Quantitative Analysis of the Effect of Hydrogen Diffusion from Silicon Oxide Etch-Stopper Layer into Amorphous In–Ga–Zn–O on Thin-Film Transistor," IEEE Transactions on Electron Devices, **61**, pp. 3762-3767 (2014) https://doi.org/10.1109/TED.2014.2359739
6. Liu X, Yan L, Yuan G, Chen L, Cheng J, Jiang C, Kong X, Chen J, Liu W, Shen W, Gang W, (2015), P-21: Effects of Low Hydrogen Dielectric Film on a-IGZO TFT Properties, *SID Symposium Digest of Technical Papers*, **46**, https://doi.org/10.1002/sdtp.10055
7. Kizu, T., Aikawa, S., Mitoma, N., Shimizu, M., Gao, X., Lin, M-F., Nabatame, T., Tsukagoshi, K., Low-temperature processable amorphous In-W-O thin-film transistors with high mobility and stability, Appl. Phys. Lett. **104**, 152103 (2014). http://dx.doi.org/10.1063/1.4871511
8. Shiah, YS., Sim, K., Shi, Y. *et al.* Mobility–stability trade-off in oxide thin-film transistors. *Nat Electron* **4**, 800–807 (2021). https://doi.org/10.1038/s41928-021-00671-0
9. Magari, Y., Kataoka, T., Yeh, W., and Furuta, M., High-mobility hydrogenated polycrystalline In2O3 (In2O3:H) thin-film transistors, Nat Commun **13**, 1078 (2022). https://doi.org/10.1038/s41467-022-28480-9
10. Ghediya, P R., Magari, Y., Sadahira, H., Endo, T., Furuta, M., Zhang, Y., Matsuo, Y., and Ohta, H., Reliable Operation in High-Mobility Indium Oxide Thin Film Transistors, Small Methods, **9**, 2400578 (2024). https://doi.org/10.1002/smtd.202400578
11. Uraoka, Y., Bermundo, J P., Fujii, M N,. Uenuma, M., and Ishikawa, Y., Degradation phenomenon in metal-oxide-semiconductor thin-film transistors and techniques for its reliability evaluation and suppression., J. Appl. Phys. **58** 090502 (2019) https://doi.org/10.7567/1347-4065/ab1604
12. Hung, M-P., Wang, D., Jiang, J., and Furuta, M., Negative Bias and Illumination Stress Induced Electron Trapping at Back-Channel Interface of InGaZnO Thin-Film Transistor, ECS Solid State Lett. **3** Q13 (2014). http://dx.doi.org/10.1149/2.010403ssl
13. Takeda, Y., Takahashi, T., Miyanaga, R., Bermundo, J-P S., Uraoka, Y., Degradation Due to Photo-Induced Electron in Top-Gate In-Ga-Zn-O Thin Film Transistors With n− Region Under Negative Bias Stress and Light Irradiation, IEEE Electron Device Letters **44**, 765 (2023). https://doi.org/10.1109/LED.2023.3258960